Identification of potential candidate genes and pathways in atrioventricular nodal reentry tachycardia by whole-exome sequencing

CLINICAL AND TRANSLATIONAL MEDICINE
Open Access

Identification of Potential Candidate Genes and Pathways in Atrioventricular Nodal Reentry Tachycardia by Whole-exome Sequencing

Journal:	*Clinical and Translational Medicine*
Manuscript ID	Draft
Wiley - Manuscript type:	Research Article
Date Submitted by the Author:	n/a
Complete List of Authors:	Luo, Rong; Chengdu Medical College Zheng, Chenqing Yang, Hao Chen, Xueping Jiang, Panpan Wu, Xiushan Yang, Zhenglin Shen, Xia Li, Xiaoping
Keywords:	AVNRT, WES, Gene-based collapsing analysis

Abstract:	Objective Atrioventricular nodal reentry tachycardia (AVNRT) is the most common form of paroxysmal supraventricular tachycardia (PSVT). Increasing data have shown familial clustering and involvement of genetic factors in AVNRT, and no pathogenic genes related to AVNRT have been reported. Methods Whole-exome sequencing (WES) was performed in 82 patients with AVNRT and 100 controls. Reference target genes, genome-wide association analysis (GWAS), gene-based collapsing and pathway enrichment analysis were performed. Protein-protein interaction (PPI) network was then established, WES database in the UK Biobank and one only genetic study of AVNRT in Denmark were used for external data validation. Results Among 129 reference target genes, 126 mutations were identified in the cases (MAF<0.001). Gene-based collapsing analysis and pathway enrichment analysis revealed six functional pathways related to AVNRT as with neuronal system/neurotransmitter release cycles and ion channel/cardiac conduction among the top 30 enriched pathways, then 36 candidate pathogenic genes were selected. By combining with PPI analysis, 10 candidate genes were identified, including RYR2, NOS1, SCN1A, CFTR, EPHB4, ROBO1, PRKAG2, MMP2, ASPH, and ABCC8. From the UK Biobank database, 18 genes from candidate genes including SCN1A, PRKAG2, NOS1, CFTR had mutations in arrhythmias, and the mutations in PIK3CB, GAD2 and HIP1R were in patients with PSVT. Moreover, one mutation of RYR2 (c.4652A>G, p.Asn1551Ser) in our study was also detected in the Danish study. Considering the gene functional roles and external data validation, the most likely candidate

	genes were SCN1A, PRKAG2, RYR2, CFTR, NOS1, PIK3CB, GAD2 and HIP1R. Conclusion The preliminary results first revealed potential candidate genes such as SCN1A, PRKAG2, RYR2, CFTR, NOS1, PIK3CB, GAD2 and HIP1R, and the pathways mediated by these genes, including neuronal system/neurotransmitter release cycles or ion channels/cardiac conduction, might be involved in AVNRT.

Identification of Potential Candidate Genes and Pathways in Atrioventricular Nodal Reentry Tachycardia by Whole-exome Sequencing

Rong Luo, PhD[1#]; Chenqing Zheng, MD[2#]; Hao Yang, MD[3] ; Xueping Chen, MD[3]; Panpan Jiang, PhD[4] ; Xiushan Wu, PhD[5]; Zhenglin Yang, PhD[3] ; Xia Shen, PhD[2, 6, 7]; Xiaoping Li, MD, PhD[3, 1 *]

1. Institute of Geriatric Cardiovascular Disease, Chengdu Medical College, 610500, People's Republic of China.

2. State Key Laboratory of Biocontrol, School of Life Sciences, Sun Yat-sen University, Guangzhou, China

3. Department of Cardiology, Hospital of the University of Electronic Science and Technology of China and Sichuan Provincial People's Hospital, Chengdu, Sichuan 610072, China

4. Shenzhen RealOmics (Biotech) Co., Ltd., Shenzhen 518081, China.

5. The Center of Heart Development, College of Life Sciences, Hunan Norma University, Changsha, China.

6. Centre for Global Health Research, Usher Institute of Population Health Sciences and Informatics, University of Edinburgh, Edinburgh, United Kingdom.

7. Department of Medical Epidemiology and Biostatistics, Karolinska Institutet, Stockholm, Sweden.

Abstract

Objective Atrioventricular nodal reentry tachycardia (AVNRT) is the most common form of paroxysmal supraventricular tachycardia (PSVT). Increasing data have shown familial clustering and involvement of genetic factors in AVNRT, and no pathogenic genes related to AVNRT have been reported.

Methods Whole-exome sequencing (WES) was performed in 82 patients with AVNRT and 100 controls. Reference target genes, genome-wide association analysis (GWAS), gene-based collapsing and pathway enrichment analysis were performed. Protein-protein interaction (PPI) network was then established, WES database in the UK Biobank and one only genetic study of AVNRT in Denmark were used for external data validation.

Results Among 129 reference target genes, 126 deleterious rare mutations in 48 genes were identified in the cases (MAF<0.001). Gene-based collapsing analysis and pathway enrichment analysis revealed six functional pathways related to AVNRT as with neuronal system/neurotransmitter release cycles and ion channel/cardiac conduction among the top 30 enriched pathways, then 36 candidate pathogenic genes were selected. By combining with PPI analysis, 10 candidate genes were identified, including *RYR2, NOS1, SCN1A, CFTR*, *EPHB4, ROBO1, PRKAG2, MMP2, ASPH,* and *ABCC8*. From the UK Biobank database, 18 genes from candidate genes including *SCN1A, PRKAG2, NOS1, CFTR* had mutations in arrhythmias, and the mutations in *PIK3CB, GAD2* and *HIP1R* were in patients with PSVT. Moreover, one mutation of *RYR2* (c.4652A>G, p.Asn1551Ser) in our study was also detected in the Danish study. Considering the gene functional roles and external data validation, the most likely candidate genes were *SCN1A, PRKAG2, RYR2, CFTR*, *NOS1, PIK3CB, GAD2* and *HIP1R*.

Conclusion The preliminary results first revealed potential candidate genes such as *SCN1A, PRKAG2, RYR2, CFTR*, *NOS1, PIK3CB, GAD2* and *HIP1R*, and the pathways mediated by these genes, including neuronal system/neurotransmitter release cycles or ion channels/cardiac conduction, might be involved in AVNRT.

Keywords: Atrioventricular nodal reentry tachycardia; whole-exome sequencing; Gene-based collapsing analysis; neurotransmitter release cycles pathway; ion channels related pathway; Ion channel genes.

Introduction

Atrioventricular nodal reentrant tachycardia (AVNRT), caused by a reentry circuit involving fast and slow atrioventricular nodal pathways, is one of the most common types of paroxysmal supraventricular tachycardias (PSVTs) [1]. Although radiofrequency ablation has a satisfactory success rate in AVNRT, the precise anatomic structures that constitute the reentrant circuit are unresolved, and the specific pathogenesis has remained the subject of study over several decades [2, 3]. Because most patients with AVNRT experience the onset of their symptoms in early adulthood and lack other structural heart disease, AVNRT was once considered a congenital functional abnormality developed during cardiogenesis [4].

However, there are several reports of AVNRT occurring in twins and members of the same family [5-8], and first-degree relatives of patients with AVNRT present a hazard ratio of at least 3.6 for exhibiting AVNRT compared with the general population [8], indicating that genetic factors are involved in the etiology and mechanism of this disease. Familial Wolff-Parkinson-White syndrome, another type of PSVT, has been well recognized as a disease that is partly caused by gene mutations, and several responsible mutations in the PRKAG2 gene have been identified [9, 10]. However, much less is known about the potential hereditary contribution to AVNRT, and no related pathogenic genes have been reported to date.

Whole-exome sequencing (WES) is an efficient strategy for identifying pathogenic genes involved in complex Mendelian and/or non-Mendelian diseases. However, factors such as lack of large multiplex families, locus heterogeneity, and incomplete penetrance have hampered such efforts to identify pathogenic genes in many diseases. Recent advances in

gene-based collapsing analysis might overcome some of these limitations [11]. In addition, rather than investigating associations between single genetic variants and a phenotype, pathway analysis of WES data interrogates alterations in biological pathways and helps us identify the underlying genes that cause disease. Therefore, we hypothesize that the application of this more comprehensive approach may help elucidate the genetic etiology of AVNRT.

To our knowledge, there are no published studies examining rare coding variants across the genome in AVNRT. In the current pilot study, we examined AVNRT using WES to detect and identify possible disease-causing genes by gene-base burden, pathway enrichment and protein-protein interaction (PPI) analyses.

Subjects and Methods

The study participants were identified among patients treated with radiofrequency catheter ablation at the Department of Cardiology of the Sichuan Academy of Medical Sciences and the Sichuan Provincial People's Hospital in the period from 2014 to 2017. A total of 100 unrelated ethnically matched healthy control subjects were recruited from the visitors to the Health Evaluation and Promotion Center of our hospital. Upon inclusion, blood sample tests, 12 lead electrocardiograms (ECGs), echocardiography and cardiac history were recorded. The control subjects were free of any cardiovascular diseases, arrhythmia, chronic anemia, diabetes mellitus, thyroid disorders, electrolyte disturbance, systemic immune diseases, malignant tumors or any other diseases known to cause arrhythmias. All subjects gave written informed consent for genetic screening. Ethical approval for this study was obtained from the ethics committee of the Sichuan

Academy of Medical Sciences and the Sichuan Provincial People's Hospital.

Intracardiac Electrophysiological Study

Baseline intracardiac electrophysiological studies included atrial stimulation (burst or extra stimulus pacing) and ventricular stimulation in cases. AVNRT diagnosis was established according to published criteria and pacing maneuvers as applicable [12]. Dual atrial ventricular (AV) node physiology was defined as a ≥50 ms increment in the AH interval after a 10 ms decrement interval during single-atrial extra stimulation or a ≥50 ms increment in the AH interval after shortening the pacing cycle length by 10 ms. If sustained AVNRT (lasting ≥30 s) was not induced, the same pacing maneuvers were repeated under isoproterenol infusion and withdrawal as previously described [13].

Next-generation DNA sequencing, Variant Calling and Annotation

DNA samples were extracted from peripheral blood using the QIAamp DNA Blood Mini and Maxi Kits (Qiagen, Hilden, Germany) according to the manufacturer's instructions. Entire exon sequences were enriched by using a SureSelect Human All Exon kit V6 (Agilent Technologies, Santa Clara, CA, USA), and the libraries were sequenced on the Illumina HiSeq NovaSeq platform (Illumina, San Diego, CA, USA). The average read depth was 123, and on average, 96.4, 98.6 and 99.4% of exons were covered by at least 20 reads, 10 reads and 4 reads, respectively (Supplement Figure-1 S15). Qualified sequence reads were aligned to the human reference genome (NCBI GRCh37) using the Burrows-Wheeler Aligner (BWA; version 0.5.17; http://bio-bwa. sourceforge. net/). SAMtools (version 0.1.18; http://samtools. sourceforge.net/), Picard (http://picard. sourceforge.net/) and GATK (http://www. broadinstitute.org/ gsa/wiki/index.php/ Home_Page) were used for removing duplicated reads, realignment, and recalibration.

Potential single nucleotide variants (SNVs) and small insertions and deletions were called and filtered by using GATK3.7. Then, high-confidence SNV and indel mutations were annotated using snpEff (Version 4.2; http://snpeff. sourceforge.net/). Furthermore, all variants were annotated according to the control population of the 1000 Genomes Project (2014 Oct release, http://www. 1000genomes. org), ExAC (http://exac.broadinstitute.org), EVS (http://evs.gs.washington. edu/EVS), and the disease databases of ClinVar (http://www. ncbi.nlm.nih. gov/clinvar) and OMIM (http://www.omim.org). Missense variants were evaluated as pathogenic variants when high damage effects were predicted by at least three out of five appropriate programs, including Sorting Intolerant from Tolerant [SIFT], Polyphen2-HDIV, MutationTaster and MutationAssessor.

Mutations in reference target genes

A total of 129 reference AVNRT target genes were selected to detect mutations in AVNRT cases and controls. The genes were selected based on the following criteria according to another pioneering study on gene mutations in AVNRT[14]: (1) PR interval-associated genes identified by genome-wide association studies [15], (2) genes selected based on cardiac expression levels [16], (3) plausible genes based on protein function and association with other arrhythmic diseases. Selected genes are listed in Supplementary Table S1.

Single-marker association analysis

We used GATK v3.7 CombineGVCFs to combine the whole-exome sequencing dataset with ethnically matched and unrelated subjects in the AVNRT cohort and the control group, followed by filtering with VQSR and PLINK1.9 (--geno 0.1 --hwe 0.0001) to obtain high-confidence variant datasets [17]. Furthermore, PLINK1.9 was applied to

check the multidimensional scaling (MDS) dataset based on raw Hamming distances for population stratification, identity by descent (IBD) calculation for sample pairs and Hardy-Weinberg equilibrium deviation for all markers. GWAS for the qualified high-confidence datasets was performed to compute the odds ratios (ORs) and *p* values in PLINK using *Fisher*'s exact test for dichotomous phenotypes (cases versus controls for AVNRT). Finally, we used a genome-wide threshold for significance of $p < 1 \times 10^{-6}$. A quantile-quantile (Q-Q) plot was used to evaluate the resulting p values.

Gene-based collapsing analysis and pathway enrichment

We performed gene-based collapsing to combine the information on multiple deleterious rare variants into a single value per gene, with ethnically matched and unrelated subjects in the AVNRT cohort (n=82) and the control group (n=100). We defined deleterious rare mutations as nonsense, splice-site, indel and frameshift mutations. For statistical considerations, Fisher's exact test methods were preferred to calculate the gene-based collapsing. Two groups with minor allele frequencies (MAFs) below 0.1% and 1% in the Exome Aggregation Consortium (ExAC) and 1000 Genomes Project databases were calculated separately. A p value < 0.05 was considered significant. The significant genes were submitted to the KOBAS3.0 web server (http://kobas.cbi.pku.edu.cn/kobas3) to obtain the functional gene set Reactome Pathway enrichment. Then, the rich factor was calculated, and the top 30 enriched pathways are shown based on the corrected *p* value.

Construction of the PPI network

The Search Tool for the Retrieval of Interacting Genes database (STRING) (Version 10.0, http://string-db.org) was used to predict the relationships among the screened genes and

identify the most relevant genes [18]. Based on experimental data, database entries, and coexpression, PPI node pairs with a score of combination >0.4 (medium confidence) were considered to be significant. Then, Cytoscape software (version 3.7.1) was used to visualize the resulting PPI network.

Results

Clinical data of the cases

Our analysis included WES data from 82 cases and 100 controls. All AVNRT patients were diagnosed by electrophysiologic examination and underwent radiofrequency ablation. Among the 82 cases included in our analyses, the mean age at symptom onset was 51.5±16.3 years old, and the ratio of females/males was 2.2:1. The median disease course was 4.0 years. Five patients had a history of syncope or approximate syncope, 3 had a familiar history or suspected familiar history of AVNRT, and no patients exhibited any structural heart disease. In the electrophysiological study, 9 patients presented no jumping between dual AV nodes, isoproterenol infusion was used in 6 cases to induce the onset of AVNRT. Except for one patient who exhibited slow-slow and one with slow-fast, all other cases exhibited typical slow-fast AVNRT, and all cases were treated successfully with radiofrequency ablation, with only one case relapsing, more details see Supplementary Table S2.

Referentially elated target gene mutations

Among the 129 reference target genes, 126 deleterious rare mutations in 48 genes were detected according to the definition of mutations with an MAF <0.001 in the ExAC and 1000 Genomes Project databases: 11 mutations in *KCNJ12* (n=11), 9 in *RYR3* (n=9), 8 in

RYR2 (n=8), 7 in *ZFHX3* (n=7), 6 in *ANK2* (n=6); 5 in *AKAP9* (n=5), *SYNE2* (n=5), *TRPM4* (n=5); 4 in *CACNA1D* (n=4), *CACNA1I* (n=4), *GNB3* (n=5), *MYH6* (n=4), *SCN5A* (n=4); 3 in *HCN4* (n=3), *KCNH2* (n=3), *SCN1A* (n=3), *SCN3A* (n=3); 2 in *CACNA1G* (n=2), *CACNB2* (n=2), *GJD3* (n=2), *NUP155* (n=2), *SCN4A* (n=2), *SCN10A* (n=2), *SYNP02L* (n=2); 1 mutation in 1 case in following genes: *ADRB2, C9orf3, CASQ2, CAV1, CAV3, ERG, HCN2, HCN3, ITPR1, KCNA4, KCNA5, KCND3, KCNN3, LMNA, PITX2, PKP2, PRKAG2, SCN1B, SCN4B, SCN9A, SLC8A1, SNTA1, SOX5* and *TBX3* (Supplementary Table S3, Figure 1). Among the above mutations in the listed genes, only 2 controls exhibited 2 mutations in *KCNJ12* and 1 mutation was found in one control subjed in each of *HCN4*, *ANK2* and *RYR2*.

As PSVT has a prevalence of 22.5/10 000 persons and an incidence of 35/100 000 person-years [19], and the sample examined in the current study was relatively small, we chose another definition of mutations with an MAF <0.01 in the ExAC and 1000 Genomes Project databases, and a total of 227 mutations in 64 genes were detected. The details of the mutations are presented in Supplementary Table S4.

GWAS study for common variants

Single-nucleotide polymorphisms (SNPs) were removed from the pre-imputation dataset if they exhibited an MAF < 0.01 or a *p* value for Hardy-Weinberg equilibrium (HWE) < 1×10^{-4} (Supplementary Figure 2). Association *p* values from the GWAS were reported in Q-Q plots and Manhattan plots (Figure 2, Supplementary Figure-2 S16). In the limited number of samples, SNPs with *p* values (*Fish* test) of less than less than 10^{-6} were shown in Supplementary Table S5.

Then, pathway enrichment was performed under the condition of including SNPs with

p<0.01 according to KEGG and Reactome databases. As shown in Figure 2, the following four related traits were among the top 30 pathways in the two databases: (1) vesicle-mediated transport; (2) axon guidance; (3) the Ca^{2+} signaling pathway; and (4) ion channel transport, and there were 20 genes in both the KEGG and Reactome database analyses, including *ABLIM2, ASPH, ATP2B4, CACNA1G, DPYSL2, EPHA2, FES, MYL12A, NE01, PLXNA4, PLXNB1, PLXNC1, ROBO2, RYR1, RYR2, RYR3, SEMA5A, SEMA6D, SLIT3* and *UNC5B* (Table 1).

Gene-based collapsing analysis and pathway enrichment for rare variants

We carried out gene-based collapsing tests under 2 frequency categories (MAF <0.01 and MAF <0.001) with *p* values of less than 0.05 were included. The Q-Q plots, Manhattan figures and mutations of the genes were shown in Supplemental Figure-3 S17 and Supplemental Tables S6 and S7.

In pathway analysis, mutations are associated with genes, and genes are placed into sets. The pathway enrichment analysis was performed using the Reactome database, and there were 517 and 343 pathways enriched with an MAF<0.01 and MAF<0.001, respectively (Supplementary Tables S8, S9). Among the top 30 enriched pathways, there were 6 related pathways (MAF <0.01) and 2 pathways related to AVNRT (MAF P<0.001) (Figure 3). In addition, 14 pathways other than the top 30 pathways exhibited potential functions associated with AVNRT with either an MAF <0.01 or MAF<0.001 (Table 2, 3).

From the above related pathways, 36 candidate pathogenic genes were selected: *ABCC8, AP1G2, ASPH, ATP2C2, BEGAIN, CD163, CFTR, COG4, COL5A1, COL4A3, CSF2RB, DOK4, EPHB4, EVL, GAD2, HEPH, HIPK2, HIP1R, KCNV2, LAMC1, LRFN4, MMP2,*

NOS1, PIK3CB, PPFIA1, PRKAG2, PSMB11, ROBO1, SCN1A, SFTPA2, SLC9B1, SLC26A4, SLC12A4, SYT10, TCF7L1 and *TSPOAP1* (Table 4). The mutant information for these candidate genes was listed in Supplemental Tables S10 and S11. Among the candidate genes, *SCN1A* and *PRKAG2* were identified in arrhythmia diseases as reference target genes.

PPI network construction and analysis

To identify the most relevant genes among the above 36 candidate genes from gene-based collapsing analysis, the PPI network was constructed with STRING, which combined 64 reference target genes with mutations from the present study and 20 selected genes among the top 30 enriched pathways according to both the KEGG and Reactome databases in a GWAS. The 9 most significant genes according to scores and nodes were *NOS1* (score=6.795, nodes=8.5), *SCN1A* (score=6.071, nodes=10.5), *CFTR* (score=4.673, nodes=6.5), *EPHB4* (score=4.483, nodes=7.5), *PRKAG2* (score=4.335, nodes=8), *ROBO1* (score=4.241, nodes=6.5), *ASPH* (score=3.001, nodes=3.5), *MMP2* (score=2.665, nodes=4) and *ABCC8* (score=2.387, nodes=4.5). Remarkably, *RYR2* (score=14.88, nodes= 23.5) was ranked as the first PPI node among the reference target genes with mutations in the present study, and the *p* value of the burden gene test was nearly 0.05 (p=0.55) with frequency categories (MAF<0.001). Considering the functional roles of the genes and previous studies, the most likely candidate genes were *SCN1A, PRKAG2, RYR2, CFTR,* and *NOS1* (Figure 4, Table 5), and the mutation information for the selected top 5 genes was illustrated in Figure 5 and listed in Supplementary Table S12.

External data validation

To verify the candidate pathogenic genes that we screened, we selected the UK Biobank resource for external data validation. The database was the most recent upload of the total exome sequencing data from 49,960 participator [20]. We searched for mutations in our candidate genes that were associated with arrhythmias in UK Biobank summary statistics database. Among these 37 candidate genes (36 genes from the gene-based collapsing analysis and *RYR2*), we obtained information about 33 mutations in 18 genes in this database of arrhythmia patients; these genes were S*CN1A, PRKAG2, CFTR, NOS1, PIK3CB, GAD2, HIP1R, ASPH, CD163, SLC9B1, ROBO1, EPHB4, KCNV2, PPFIA1, SYT10, COG4, MMP2* and *CSF2RB*. In particular, mutations in three genes, *PIK3CB, GAD2* and *HIP1R*, were present even in patients with PSVT (Figure 6, Table 6, Supplementary Table S13). To explore the certain phenotype which burden gene were most correlative, the enrichment analysis showed these three burden genes are most significant enriched in PSVT (p=0.000174) from 791 phenotypes category in UK Biobank (Figure 6, Table 7, Supplementary Table S14).

Because the disease information of UK Biobank was not specific enough, we chose the only known AVNRT genetic sequencing study to further validate our candidate pathogenic genes. The study, published in 2018, was carried out in Denmark, and 67 known arrhythmia target genes were detected in AVNRT cases by next-generation sequencing[14]. Among our candidate genes, *SCN1A, RYR2* and *PRKAG2*, there were 11 mutations in *SCN1A* and 3 mutations in *RYR2* detected in AVNRT patients in the Danish study, especially, a mutation in *RYR2* (c.4652A>G, p.Asn1551Ser, rs185237690) in our present study was also found in one Danish AVNRT case, which supports *SCN1A* and *RyR2* gene as candidate pathogenic genes in our study. The detail mutations information

shown in Table 8.

Discussion

This is, to our knowledge, the first study with the primary aim of investigating the genetic component of AVNRT using a WES approach. In the present study and an external data validation, genes such as *SCN1A, PRKAG2, RYR2, CFTR*, *NOS1, PIK3CB, GAD2* and *HIP1R*, responsible for neuronal system/neurotransmitter release or ion channel/cardiac conduction, are likely to be candidate genes and pathways for AVNRT. As this is only the beginning of the genetic investigation of AVNRT, further genetic functional studies are needed.

Recently, an increasing number of clinical reports have suggested that there may be a hereditary contribution to AVNRT [5-8]. However, much less is known about the hereditary contribution to AVNRT compared with that for Wolff-Parkinson-White syndrome[9, 10]. A recent study involving the sequencing of 67 selected genes associated with arrhythmia in 298 AVNRT patients found the greatest number of mutations in sodium and calcium channels, indicating that AVNRT might be an electrical arrhythmic disease with abnormal sodium and calcium handling [14]. Among the reference target genes from the present study, many mutations were detected in *KCNJ12, RYR3, RYR2, ZFHX3, ANK2, AKAP9, GNB3, SYNE2, CACNA1D, CACNA1I, GNB3, MYH6, SCN5A, SCN1A, SCN3A, HCN4* and *KCNH2*. Most of these genes, such as *KCNJ12, RYR3*, *RYR2, CACNA1D, CACNA1I, SCN5A, SCN1A, SCN3A, HCN4* and *KCNH2,* encode ion channels, indicating that AVNRT was associated with ion channels. Interestingly, the causal gene of Wolff-Parkinson-White syndrome, *PRKAG2*, was also identified in our AVNRT cases.

The autonomic nervous system is known to play an important role in the triggering and termination of AVNRT [21-24]. There are extrinsic and intrinsic components of the cardiac autonomic nervous system, and the extrinsic component is divided into sympathetic and parasympathetic systems, involving the main neurotransmitters of norepinephrine and acetylcholine, respectively [25, 26]. The intrinsic cardiac autonomic nervous system of the ganglionated plexi (GP) contains both sympathetic and parasympathetic fibers and is connected with a wide range of neurotransmitters [27, 28]. The AV node exhibits dense parasympathetic innervation, and changes in the cardiac autonomic nervous system could lead to arrhythmias [29]. Usually, sympathetic stimulation is used to facilitate the induction of AVNRT [21, 22]. However, the onset of AVNRT occurs at times of increased vagal tone, as the vagal tone increases the refractory period of the fast pathway, and a premature atrial complex may be conducted antegrade via the slow pathway with subsequent retrograde conduction, thus initiating AVNRT [23, 24]. In our present study, many mutations in genes involved in the neurotransmitter release cycle and neuronal system pathways, such as the neurotransmitter release cycle, acetylcholine neurotransmitter release cycle, serotonin neurotransmitter release cycle, and norepinephrine neurotransmitter release cycle, were present among the top 30 enriched pathways, the similar outcomes were also presented in GWAS analysis, indicating that neurotransmitter release affects the sympathetic or parasympathetic system and then induces AVNRT.

The autonomic nervous system also shows a close relationship with cardiac ionic conductance. Vagal nerve endings release acetylcholine, activate the ACh-activated K1 current (IK, ACh) and inhibit the funny current (If) and the L-type Ca^{2+} current [30]. In

contrast, sympathetic nerve endings release noradrenaline to increase the If and the L-type Ca^{2+} current and induce changes in intracellular Ca^{2+} handling[31]. In addition, many arrhythmias occur due to genetic mutations in ion channels themselves, and the mutations will affect the sodium, potassium, and calcium channels responsible for ion transport across the myocardial cell membrane. Then, the action potential is altered and induces arrhythmias [32-34]. In the present study, the pathways of ion channels and cardiac conduction were among the top 30 enriched pathways, and genes such as those encoding sodium channels (*SCN1A*) and potassium channels (*KCNV2*) were selected as candidate genes; in particular, *SCN1A* is regarded as one of the most likely candidate pathogenic genes. Mutations in ion channel genes might affect the conduction of AV nodes, and differences in conduction velocity will lead to dual AV node physiology and AVNRT.

There were three genes with mutations reported to be associated with arrhythmia among the candidate genes in the present study. The first was the *PRKAG2* gene, encoding the gamma2 regulatory subunit of adenosine monophosphate- activated protein kinase (AMPK), which was identified as the pathogenic gene of Wolff-Parkinson-White syndrome [9, 10]. *PRKAG2* mutations induce the slowing of sodium channel inactivation and increase the likelihood of channel activation at more negative potentials [35]. The integral of the sodium current (total inward current) is a major determinant of conduction velocity, and increases in inward sodium current can speed up this process, resulting in a conduction velocity change in the AV node[36]. The second gene was *SCN1A*, which is primarily a neuronal gene. Nav1.1, a product of *SCN1A*, is present in various regions of the heart [37, 38]. *SCN1A* mutations are found in up to 80% of patients with Dravet

syndrome, a type of epilepsy observed in infancy, and sudden unexpected death results in 38% of all deaths in patients with a childhood onset [39]. Although the mechanism remains poorly understood, the sodium channel-dependent cardiac current is increased in *SCN1A-R1407X* knock-in mice [40], and autonomic dysfunctions such as abnormalities in heart rate variability (HRV), QT and P wave dispersion are observed in patients with Dravet syndrome [41], suggesting that some *SCN1A* variants might cause sudden death or lethal arrhythmia through neurocardiac or solely cardiac mechanisms. The third gene was *RYR2*, encoding cardiac ryanodine receptors (RyR2s), which are large intracellular Ca^{2+} channels that control the release of Ca^{2+} from the sarcoplasmic reticulum in cardiomyocytes[42]. Mutations in *RYR2* can increase the probability of channel open during diastole, resulting in excess diastolic SR Ca^{2+} release, and the increased SR Ca^{2+} leak during diastole can increase the frequency of spontaneous Ca^{2+} sparks, resulting in an untimely depolarizing inward current that triggers delayed after depolarizations and ventricular arrhythmia or atrial fibrillation [42, 43]. As mutations in these three genes have been proven to cause arrhythmia by experimental and clinical data, and were verified by the external data of UK Biobank and the genetic study from Denmark, it is reasonable for us to assume that the gene mutations identified in the present study could also cause AVNRT.

Among the other two candidate genes, the first was *CFTR*. It encodes a cAMP-activated chloride channel (cystic fibrosis transmembrane conductance regulator, CFTR) and is expressed mainly in epithelial cells of the respiratory and digestive tracts; mutations in this gene cause cystic fibrosis [44]. Subsequent studies demonstrated that CFTR acts not only as an ATP-gated chloride channel but also as a regulator of other ion channels, such

as amiloride-sensitive Na^+ channels, ATP channels and inward rectifier K^+ channels [45-47]. Recently, in cardiac CFTR-overexpressing mice, intracardiac electrophysiological studies showed marked slowing of conduction parameters, including high-grade AV block, with easily inducible non-sustained ventricular tachycardia following isoproterenol administration [48]. The second of these genes was *NOS1*. It encodes neuronal nitric oxide synthase (nNOS) and is a major isoform within the brain [49]. nNOS, together with its adaptor protein (CAPON), is also found in both intrinsic cardiac vagal neurons and postganglionic sympathetic neurons of the stellate ganglia [50, 51]. Moreover, the overexpression of nNOS increases acetylcholine release [52], and CAPON overexpression in myocytes attenuates the L-type calcium current, slightly increases the rapid delayed rectifier current (IKr), and shortens action potentials [53], which causes arrhythmia susceptibility. Thus, although the two candidate genes *CFTR* and *NOS1* have not been proven to directly cause arrhythmia, all the potential evidence listed above shows that these gene mutations can change some characteristics of atrioventricular node conduction by affecting the autonomic nervous system/neurotransmitter release or ion channels, which can lead to changes in cardiac depolarization, action potentials, cardiac conduction velocity, the refractory period, etc., and such changes will lead to dual AV node physiology and AVNRT.

As for the three candidate genes, *PIK3CB, GAD2* and *HIP1R*, were present even in patients with PSVT in the UK Biobank resource. However, there were no data showed any roles of them in the arrythmia. *PIK3CB* encodes an isoform of the catalytic subunit of phosphoinositide 3-kinase beta (PI3K β), recent data showed PI3K signaling activation affected currents of multiple ion channels, including calcium and sodium channels, and

suppression of PI3K activation displayed a prolonged QT interval [54]. *GAD2* is a glutamate decarboxylase 2 coding gene, diseases associated with *GAD2* include autoimmune polyendocrine syndrome and stiff-person syndrome, among its related pathways are neurotransmitter release cycle and database. Diseases associated with *HIP1R* (Huntingtin Interacting Protein 1 Related) include expressive language disorder and cataract. At present, there is a lack of data about the three gene mutations in arrhythmia or AVNRT, which needs to be confirmed by other large samples genetic research or functional verification

Limitations

The major limitation of the current study is the small sample size as AVNRT with low prevalence in population. When studying rare variants, larger samples are needed to adequately show that certain genes or variants are associated with the disorder. Although we identified a few candidate genes, such as *SCN1A, PRKAG2, RYR2, CFTR*, *NOS1, PIK3CB, GAD2* and *HIP1R,* in AVNRT in the present study, the genes were not verified experimentally, and further research is needed to explore the potential mechanisms of these genes. Since AVNRT is caused by complex molecular mechanisms, a single pathway is not sufficient to explain the pathogenesis of this disease. Therefore, further experimental research is needed to confirm the current findings. Finally, the controls included in the present study did not undergo invasive electrophysiological examination, and it is possible that the controls were not completely devoid of AVNRT.

Conclusions

Our study identified a number of potentially disease-related genes, such as *SCN1A, PRKAG2, RYR2, CFTR*, *NOS1, PIK3CB, GAD2* and *HIP1R,* in the pathways of neuronal system/neurotransmitter release cycles or ion channel/cardiac conduction, which require further replication in larger cohorts and functional confirmation. Because the anatomic substrate in AVNRT remains unclear, our findings may provide insight into the molecular basis of AVNRT and provide a new view of AVNRT.

Conflicts of interest

The authors report no conflicts of interest. The authors alone are responsible for the content and writing of this article. The manuscript has been approved by the responsible authorities of the institutions where the work was conducted, and all authors have read the manuscript and approved its submission to your journal.

Funding

This work was supported by National Natural Science Foundation of China (No. 81770379, 81500297 and 81470521).

References

1. Akhtar M, Jazayeri MR, Sra J, Blanck Z, Deshpande S, Dhala A. Atrioventricular nodal reentry: Clinical, electrophysiological, and therapeutic considerations. Circulation 1993; 88:282-295.

2. McGuire MA, Janse MJ. New insights on anatomical location of components of the reentrant circuit and ablation therapy for atrioventricular junctional reentrant tachycardia. *Curr Opin Cardiol*. 1995;10:3-8.

3. Wu J, Zipes DP. Mechanisms underlying atrioventricular nodal conduction and the reentrant circuit of atrioventricular nodal reentrant tachycardia using optical mapping. *J Cardiovasc Electrophysiol*. 2002;13:831-834.

4. McGuire MA, Janse MJ. New insights on anatomical location of components of the reentrant circuit and ablation therapy for atrioventricular junctional reentrant tachycardia. *Curr Opin Cardiol*. 1995;10:3-8.

5. Lu CW, Wu MH, Chu SH. Paroxysmal supraventricular tachycardia in identical twins with the same left lateral accessory pathways and innocent dual atrioventricular pathways. Pacing Clin Electrophysiol. 2000, 23:1564-1566.

6. Hayes JJ, Sharma PP, Smith PN, Vidaillet HJ. Familial atrioventricular nodal reentry tachycardia. Pacing Clin Electrophysiol. 2004, 27:73-76.

7. Namgung J, Kwak JJ, Choe H, Kwon SU, Doh JH, Lee SY, et al. Familial occurrence of atrioventricular nodal reentrant tachycardia in a mother and her son. *Korean Circ J*. 2012;42:718-721.

8. Michowitz Y, Anis-Heusler A, Reinstein E, Tovia-Brodie O, Glick A, Belhassen B. Familial occurrence of atrioventricular nodal reentrant tachycardia. Circ Arrhythm

Electrophysiol. 2017;10:e004680.

9. Gollob MH, Green MS, Tang AS, Gollob T, Karibe A, Ali Hassan AS, et al. Identification of a gene responsible for familial Wolff-Parkinson-White syndrome. N Engl J Med. 2001,344:1823-31.

10. Gollob MH, Seger JJ, Gollob TN, Tapscott T, Gonzales O, Bachinski L, et al. Novel PRKAG2 mutation responsible for the genetic syndrome of ventricular preexcitation and conduction system disease with childhood onset and absence of cardiac hypertrophy. Circulation. 2001, 104:3030-3033.

11. Moutsianas L, Agarwala V, Fuchsberger C, Flannick J, Rivas MA, Gaulton KJ, et al. The power of gene-based rare variant methods to detect disease-associated variation and test hypotheses about complex disease. PLoS Genet. 2015, 11(4):e1005165.

12. Knight BP, Ebinger M, Oral H, Kim MH, Sticherling C, Pelosi F, et al. Diagnostic value of tachycardia features and pacing maneuvers during paroxysmal supraventricular tachycardia. *J Am Coll Cardiol*. 2000; 36: 574-582.

13. Topilski I, Rogowski O, Glick A, Viskin S, Eldar M, Belhassen B. Radiofrequency ablation of atrioventricular nodal reentry tachycardia: a 14 year experience with 901 patients at the Tel Aviv Sourasky Medical Center. Isr Med Assoc J. 2006, 8:455-459.

14. Andreasen L, Ahlberg G, Tang C, Andreasen C, Hartmann JP, Tfelt-Hansen J, et al. Next-generation sequencing of AV nodal reentrant tachycardia patients identifies broad spectrum of variants in ion channel genes. Eur J Hum Genet. 2018, 26(5):660-668.

15. Pfeufer A, van Noord C, Marciante KD, Arking DE, Larson MG, Smith AV, et al. Genome-wide association study of PR interval. Nat Genet. 2010, 42:153-159.

16. Greener ID, Monfredi O, Inada S, Chandler NJ, Tellez JO, Atkinson A, et al. Molecular architecture of the human specialised atrioventricular conduction axis. J Mol Cell Cardiol. 2011; 50:642-651.

17. Chang CC, Chow CC, Tellier LC, Vattikuti S, Purcell SM, Lee JJ. Second-generation PLINK: rising to the challenge of larger and richer datasets. Gigascience. 2015, 4: 7.

18. Szklarczyk D, Franceschini A, Wyder S, Forslund K, Heller D, Huerta-Cepas J, et al. STRING v10: protein-protein interaction networks, integrated over the tree of life. Nucleic Acids Res. 2015; 43: D447- D452.

19. Orejarena LA, Vidaillet H Jr, DeStefano F, Nordstrom DL, Vierkant RA, Smith PN, Hayes JJ. Paroxysmal supraventricular tachycardia in the general population. J Am Coll Cardiol. 1998, 31:150-157.

20. Zhao Z, Bi W, Zhou W, VandeHaar P, Fritsche LG, Lee S. UK Biobank Whole-Exome Sequence Binary Phenome Analysis with Robust Region-Based Rare-Variant Test. American Journal of Human Genetics. 2020, 106, 3-12.

21. Huycke EX, Lai WT, Nguyen NX, et al. Role of intravenous isoproterenol in the electrophysiologic induction of atrioventricular node reentrant tachycardia in patients with dual atrioventricular node pathways. Am J Cardiol. 1989, 64:1131-1137.

22. Huycke EC, Lai WT, Nguyen NX, Keung EC, Sung RJ. Effects of isoproterenol in facilitating induction of slow-fast atrioventricular nodal reentrant tachycardia. Am J Cardiol. 1996; 78: 1299- 1302.

23. Kariyanna PT, Jayarangaiah A, Yurevich O, Francois J, Yusupov D, Zhyvotovska A, et al. Atrioventricular Nodal Reentrant Tachycardia Triggered by Marijuana Use: A Case Report and Review of the Literature. Am J Med Case Rep. 2019 ; 7(9): 193-196.

24. Chiou CW, Chen SA, Kung MH, Chang MS, Prystowsky EN. Prystowsky. Effects of Continuous Enhanced Vagal Tone on Dual Atrioventricular Node and Accessory Pathways. Circulation. 2003;107:2583-2588.

25. Triposkiadis F, Karayannis G, Giamouzis G, Skoularigis J, Louridas G, Butler J. The sympathetic nervous system in heart failure physiology, pathophysiology, and clinical implications. J Am Coll Cardiol. 2009, 54, 1747-1762.

26. Wang H, Lu Y, Wang Z. Function of cardiac M3 receptors. Auton Autacoid Pharmacol. 2007, 27, 1-11.

27. Herring N. Autonomic control of the heart: going beyond the classical neurotransmitters. Exp Physiol. 2015, 100(4):354-358.

28. Herring N, Cranley J, Lokale MN, Li D, Shanks J, Alston EN, et al. The cardiac sympathetic co-transmitter galanin reduces acetylcholine release and vagal bradycardia: implicationsfor neural control of cardiac excitability. J Mol Cell Cardiol. 2012, 52: 667 -676.

29. Franciosi S, Perry FKG, Roston TM, Armstrong KR, Claydon VE, Sanatani S. The role of the autonomic nervous system in arrhythmias and sudden cardiac death. Auton Neurosci. 2017, 205, 1-11.

30. Zhang H, Holden AV, Noble D, Boyett MR. Analysis of the chronotropic effect of acetylcholine on sinoatrial node cells. J Cardiovasc Electrophysiol. 2002, 13:465-474.

31. Zhang H, Butters T, Adeniran I, Higham J, Holden AV, Boyett MR, et al. Modeling the chronotropic effect of isoprenaline on rabbit sinoatrial node. Front Physiol. 2012, 3:241.

32. Watanabe H, Darbar D, Kaiser DW, Jiramongkolchai K, Chopra S, Donahue BS, et al.

Mutations in sodium channel beta 1 and beta 2 subunits associated with atrial fibrillation. Circ Arrhythm Electrophysiol. 2009, 2:268-275

33. Schmitt N, Grunnet M, Olesen SP. Cardiac potassium channel subtypes: new roles in repolarization and arrhythmia. Physiol Rev. 2014, 94:609-53.

34. Catterall WA. Structure and regulation of voltagegated Ca^{2+} channels. Annu Rev Cell Dev Biol. 2000;16:521-555.

35. Light PE, Wallace CH, Dyck JR. Constitutively Active Adenosine Monophosphate-Activated Protein Kinase Regulates Voltage-Gated Sodium Channels in Ventricular Myocytes. Circulation. 2003;107:1962-1965.

36. Kucera JP, Rohr S, Rudy Y. Localization of sodium channels in intercalated disks modulates cardiac conduction. Circ Res. 2002, 91:1176-1182.

37. Lei M, Jones SA, Liu J, Lancaster MK, Fung SS, Dobrzynski H, et al. Requirement of neuronal- and cardiac-type sodium channels for murine sinoatrial node pacemaking. J Physiol. 2004, 559:835-848.

38. Maier SK, Westenbroek RE, Yamanushi TT, Dobrzynski H, Boyett MR, Catterall WA, et al. An unexpected requirement for brain-type sodium channels for control of heart rate in the mouse sinoatrial node. Proc Natl Acad Sci USA. 2003, 100: 3507- 3512.

39. Sillanpaa M, Shinnar S. Long-term mortality in childhood-onset epilepsy. N Engl J Med. 2010;363(26):2522–2529.

40. Auerbach DS, Jones J, Clawson BC, Offord J, Lenk GM, Ogiwara I, et al. Altered cardiac electrophysiology and SUDEP in a model of Dravet syndrome. PLoS ONE. 2013;8:e77843.

41. Delogu AB, Spinelli A, Battaglia D, Dravet C, De Nisco A, Saracino A, et al.

Electrical and autonomic cardiac function in patients with Dravet syndrome. Epilepsia. 2011, 52 Suppl 2:55-58

42. Eisner DA, Caldwell JL, Kistamás K, Trafford AW. Calcium and Excitation-Contraction Coupling in the Heart. Circ Res. 2017, 121(2):181-195.

44. Pizzale S, Gollob MH, Gow R, Birnie DH. Sudden death in a young man with catecholaminergic polymorphic ventricular tachycardia and paroxysmal atrial fibrillation. J Cardiovasc Electrophysiol. 2008, 19(12):1319-21.

45. Riordan JR, Rommens JM, Kerem B, Alon N, Rozmahel R, Grzelczak Z, et al. Identification of the cystic fibrosis gene: cloning and characterization of complementary DNA. Science. 1989, 245(4922):1066-73.

46. Stutts MJ, Canessa CM, Olsen JC, Hamrick M, Cohn JA, Rossier BC, et al. CFTR as a cAMP-dependent regulator of sodium channels.Science. 1995, 269 (5225): 847-850.

48. Sugita M, Yue Y, Foskett JK. CFTR Cl^- channel and CFTR-associated ATP channel: distinct pores regulated by common gates. EMBO J. 1998, 17(4):898-908.

47. Yoo D, Flagg TP, Olsen O, Raghuram V, Foskett JK, Welling PA. Assembly and trafficking of a multiprotein ROMK (Kir 1.1) channel complex by PDZ interactions. J Biol Chem. 2004, 279:6863-6873.

48. Ye L, Zhu W, Backx PH, Cortez MA, Wu J, Chow YH, et al. Arrhythmia and sudden death associated with elevated cardiac chloride channel activity. J Cell Mol Med. 2011, 15 (11):2307-2316.

49. Dawson TM, Snyder SH. Gases as biological messengers: nitric oxide and carbon monoxide in the brain. J Neurosci. 1994, 149:5147-5159.

50. Herring N, Golding S, Paterson DJ. Pre-synaptic NO-cGMP pathway modulates

vagal control of heart rate in isolated adult guinea pig atria. J Mol Cell Cardiol. 2000, 32:1795-1804.

51. Schwarz P, Diem R, Dun NJ, Forstermann U. Endogenous and exogenous nitric oxide inhibits norepinephrine release from rat heart sympathetic nerves. Circ Res.1995, 77: 841- 848.

52. Dawson TA, Li D, Woodward T, Barber Z, Wang L, Paterson DJ. Cardiac cholinergic NO-cGMP signaling following acute myocardial infarction andnNOS gene transfer. Am J Physiol Heart Circ Physiol. 2008, 295:H990-998.

53. Chang KC, Barth AS, Sasano T, Kizana E, Kashiwakura Y, Zhang Y, et al. CAPON modulates cardiac repolarization via neuronal nitric oxide synthase signaling in the heart. Proc Natl Acad Sci USA. 2008, 105:4477-4482.

54. Lu Z , Wu CY, Jiang YP, Ballou LM, Clausen C, Cohen IS, et al. Suppression of phosphoinositide 3-kinase signaling and alteration of multiple ion currents in drug-induced long QT syndrome. Sci Transl Med. 2012 Apr 25;4(131):131ra50.

Figure legends

Figure 1 The number of mutations and cases in referential target genes (A, MAF<0.01; B, MAF<0.001).

Figure 2 Manhattan plot (A) and pathway enrichment analysis of KEGG (B) and Reactome (C).

Figure 3 The top 30 pathways in Reactome pathway enrichment

Figure 4 Protein-protein interaction network. (A) The interaction network between the 36 candidate genes in gene-based collapsing analysis and the 64 reference target genes with mutations in the present study. (B) The interaction network between the 37 candidate genes (including *RYR2*) in gene-based collapsing analysis and the genes selected by pathway enrichment analysis in GWAS. (C) The interaction network with the genes selected by (A) and (B).

Figure 5 The mutations in the 5 candidate genes such as *SCN1A, PRKAG2, RYR2, CFTR* and *NOS1*.

Figure 6 Verification of candidate 37 genes in UK Biobank (A); The three of candidate burden genes, *PIK3CB, GAD2* and *HIP1R*, showed the most significant enrichment in PSVT (*p=0.000174*) among 791 phenotypes in UK Biobank (B).

Figure. 1

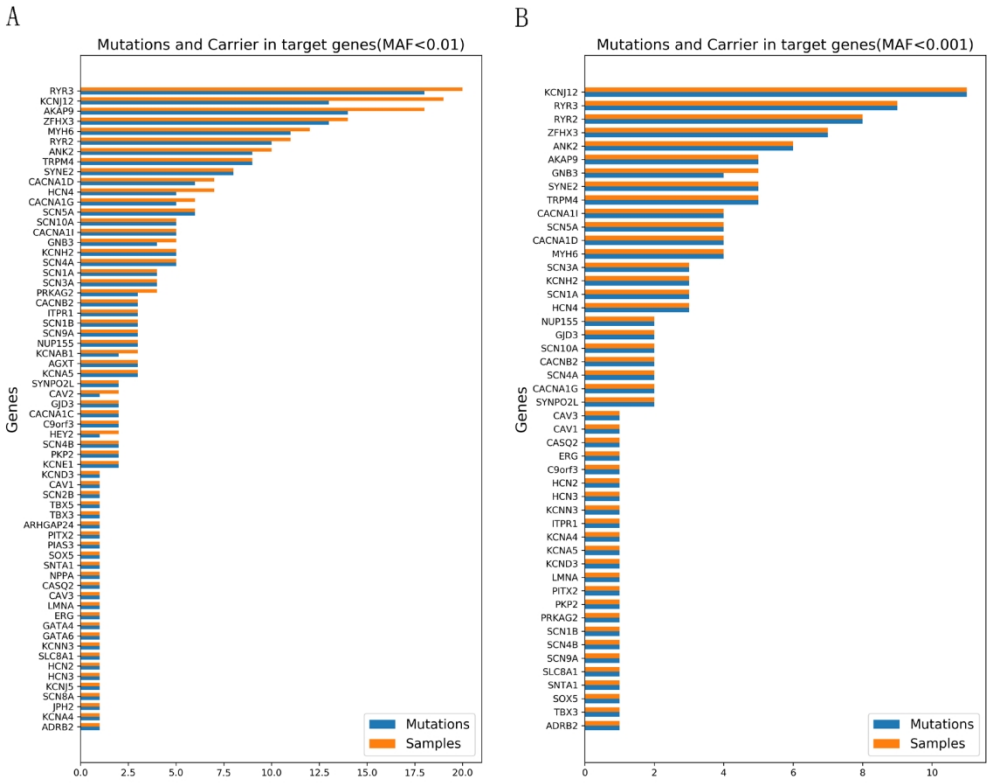

The number of mutations and cases in referential target genes

166x140mm (300 x 300 DPI)

Figure. 2

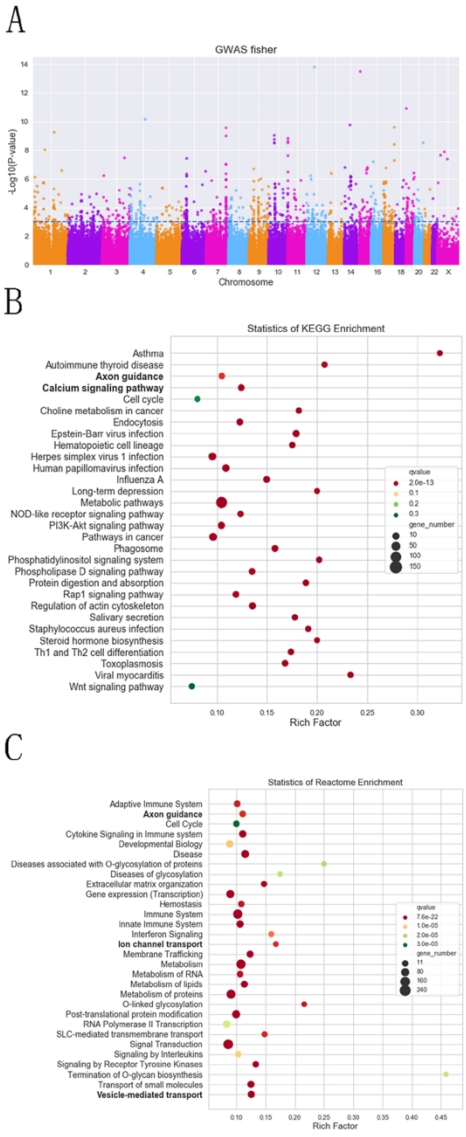

Manhattan plot (A) and pathway enrichment analysis of KEGG (B) and Reactome (C).

166x420mm (300 x 300 DPI)

Figure. 3

A

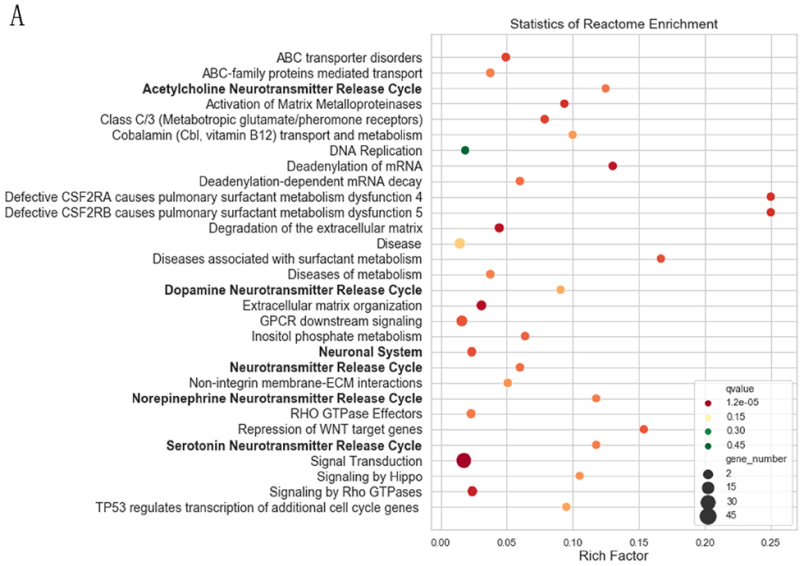

B

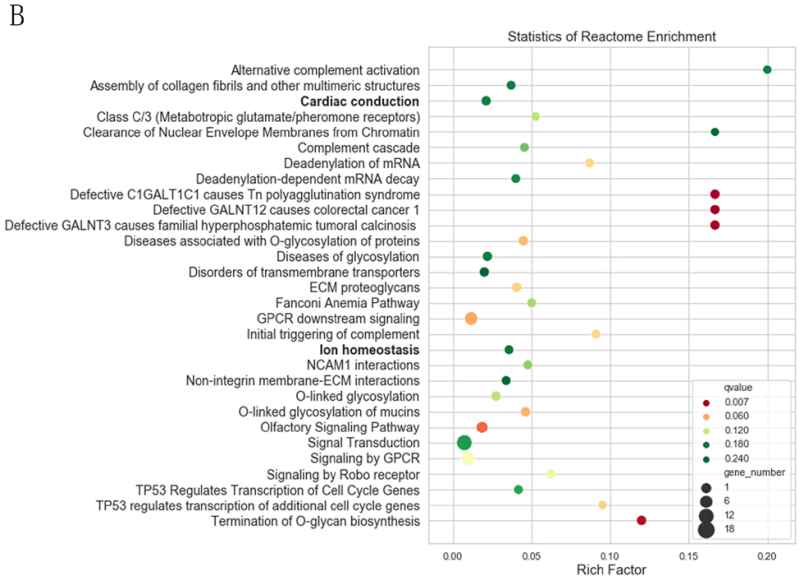

The top 30 pathways in Reactome pathway enrichment

82x123mm (300 x 300 DPI)

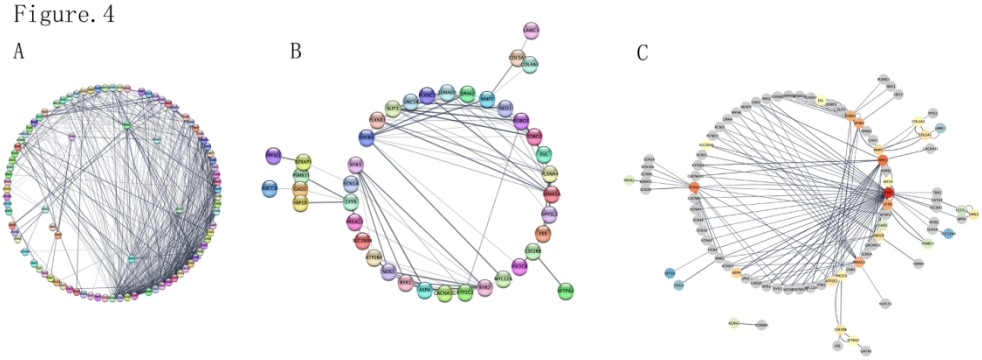

Protein-protein interaction network.

166x62mm (300 x 300 DPI)

Figure. 5

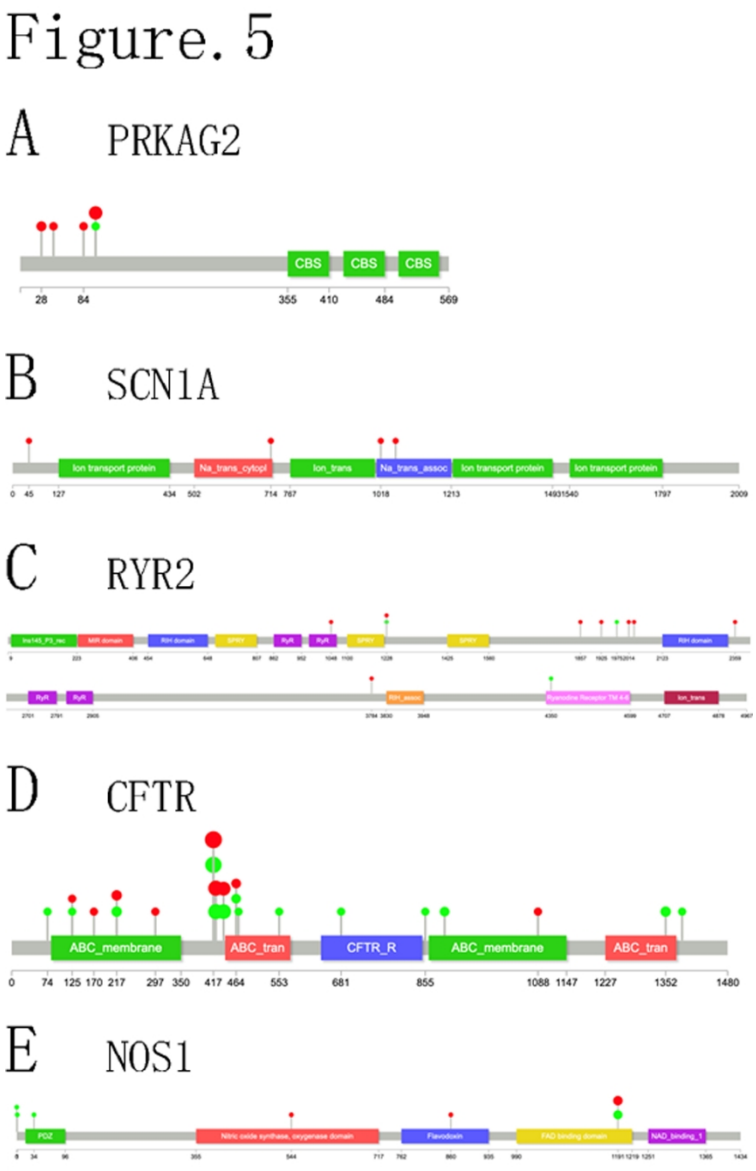

The mutations in the 5 candidate genes such as SCN1A, PRKAG2, RYR2, CFTR and NOS1.

82x133mm (300 x 300 DPI)

Figure. 6

A

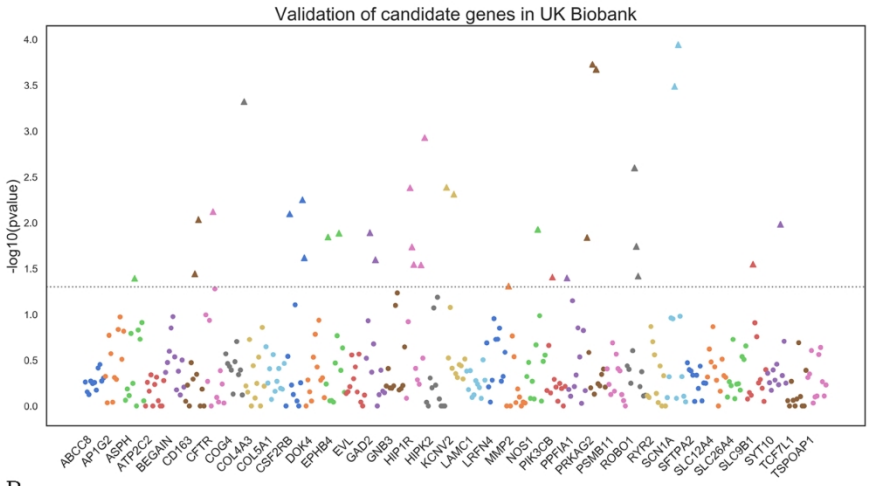

B

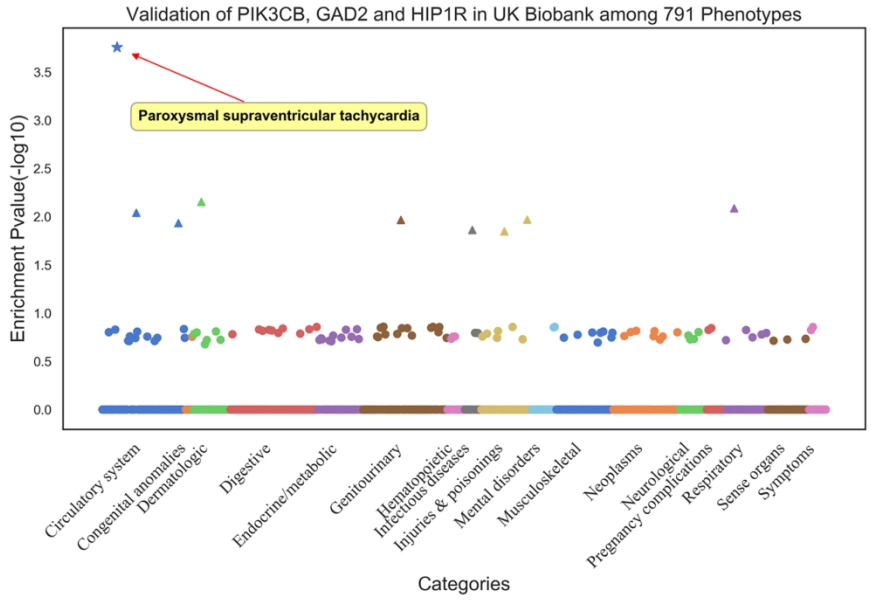

Verification of candidate 37 genes in UK Biobank

166x230mm (260 x 260 DPI)

Table 1 SNPs in genes from the pathway enrichment analysis according to both KEGG and Reactome

Genes	A1	F_A	F_U	A2	*P*	OR	Functions	Hgv.c	Hgv.p
SEMA6D	G	0.414	0.225	T	1.10E-4	2.44	Intron variant	c.1646+105G>T	.
ROBO2	G	0.207	0.075	C	3.18E-4	3.23	Intron variant	c.109+121G>C	.
MYL12A	C	0.161	0.041	CGT	3.48E-4	4.51	Intron variant	c.199+192_199+193delGT	.
ABLIM2	T	0.177	0.345	C	3.49E-4	0.41	Intron variant	c.838-131G>A	.
ATP2B2	G	0.000	0.060	A	7.05E-4	0.00	Intron variant	c.397+71C>T	.
ATP2B2	A	0.110	0.025	G	1.02E-3	4.81	Synonymous variant	c.1626C>T	p.Ile542Ile
ATP2B2	T	0.110	0.025	C	1.02E-3	4.81	Intron variant	c.1659+102G>A	.
UNC5B	T	0.120	0.027	C	1.05E-3	4.89	Intron variant	c.305-277C>T	.
NEO1	C	0.342	0.195	T	1.80E-3	2.14	Intron variant	c.1511+90T>C	.
NEO1	TA	0.348	0.200	T	1.90E-3	2.13	3-prime UTR variant	c.*52_*53insA	.
ATP2B2	T	0.183	0.325	G	2.62E-3	0.47	Intron variant	c.1417-186C>A	.
NEO1	G	0.342	0.200	A	2.77E-3	2.07	Synonymous variant	c.1779A>G	p.Lys593Lys
ASPH	C	0.518	0.359	A	2.80E-3	1.93	Intron variant	c.1108-121T>G	.
ABLIM2	A	0.232	0.380	G	3.07E-3	0.49	Intron variant	c.915+26C>T	.
PLXNB1	A	0.043	0.000	G	3.51E-3		Non-coding transcript exon variant	n.5120C>T	.
DPYSL2	T	0.108	0.028	C	3.56E-3	4.22	Intron variant	c.936+251C>T	.
PLXNC1	T	0.043	0.000	C	3.65E-3		Intron variant	c.1062+161C>T	.
CACNA1G	CTGTGTGGTGTTTGT G	0.049	0.140	C	4.41E-3	0.32	Intron variant	c.5782-165_5782-164insTGTGTGTGTGTTTGTG	.
ASPH	C	0.488	0.340	G	5.26E-3	1.85	Intron variant	c.1346-79C>G	.
UNC5B	T	0.134	0.050	C	5.31E-3	2.94	Splice region variant	c.732C>T	p.Tyr244Tyr
UNC5B	A	0.134	0.050	G	5.31E-3	2.94	Intron variant	c.734-173G>A	.
UNC5B	G	0.134	0.050	A	5.31E-3	2.94	Missense variant	c.724A>G	p.Ile242Val
UNC5B	CTG	0.134	0.050	C	5.31E-3	2.94	Intron variant	c.1100-35_1100-34insTG	.
UNC5B	T	0.134	0.050	C	5.31E-3	2.94	Intron variant	c.901+33C>T	.
ASPH	T	0.512	0.365	C	5.67E-3	1.83	Intron variant	c.1195-57G>A	.
UNC5B	A	0.128	0.045	G	6.47E-3	3.12	Intron variant	c.80-87G>A	.
EPHA2	CAG	0.041	0.000	C	6.82E-3		Intron variant	c.86-344_86-343dupCT	.
RYR3	C	0.073	0.015	G	6.92E-3	5.18	Synonymous variant	c.2403G>C	p.Leu801Leu
RYR3	G	0.073	0.015	A	6.92E-3	5.18	Intron variant	c.3556+34A>G	.

RYR2	A	0.061	0.010	G	7.78E-3	6.43	Intron variant	c.13317+48G>A	.
RYR3	C	0.370	0.240	G	7.95E-3	1.86	Intron variant	c.5861-174C>G	.
PLXNA4	CACACAACAAACAT	0.024	0.095	C	8.05E-3	0.24	Intron variant	c.3874+275_3874+276insATGTTTGTGTGT	.
SEMA5A	C	0.352	0.223	T	8.65E-3	1.89	Intron variant	c.1599+327G>A	.
RYR1	G	0.012	0.070	A	8.74E-3	0.17	Intron variant	c.11689+68A>G	.
SLIT3	G	0.253	0.383	A	9.35E-3	0.55	Intron variant	c.1459+4296C>T	.
RYR2	G	0.438	0.299	A	9.66E-3	1.82	Intron variant	c.9128+133A>G	.
FES	T	0.037	0.11	C	9.71E-3	0.31	Non coding transcript exon variant	n.616T>C	.
FES	A	0.037	0.11	G	9.71E-3	0.31	Intron variant	c.388-212A>G	.

Notes: A1, Allele 1 (usually minor); FA, Allele 1 frequency among cases; FU, Allele 1 frequency among controls; hgv.c: human genome variation c.DNA; hgv.p: human genome variation protein.

Table 2 Gene-based pathway enrichment according to Reactome (MAF < 0.01)

Pathways	ID	Input number	Background number	*P*-Value	Corrected *P*-Value	Genes
Neuronal System	R-HSA-112316	8	339	0.004	0.048	*ABCC8, PPFIA1, LRFN4, TSPOAP1, BEGAIN, GAD2, SYT10, KCNV2*
Neurotransmitter Release Cycle	R-HSA-112310	3	50	0.007	0.064	*TSPOAP1, PPFIA1, GAD2*
Acetylcholine Neurotransmitter Release Cycle	R-HSA-264642	2	16	0.008	0.068	*TSPOAP1, PPFIA1*
Serotonin Neurotransmitter Release Cycle	R-HSA-181429	2	17	0.008	0.072	*TSPOAP1, PPFIA1*
Norepinephrine Neurotransmitter Release Cycle	R-HSA-181430	2	17	0.008	0.072	*TSPOAP1, PPFIA1*
Dopamine Neurotransmitter Release Cycle	R-HSA-212676	2	22	0.013	0.096	*TSPOAP1, PPFIA1*
Glutamate Neurotransmitter Release Cycle	R-HSA-210500	2	23	0.014	0.100	*TSPOAP1, PPFIA1*
Axon guidance	R-HSA-422475	9	549	0.023	0.133	*EPHB4, LAMC1, MMP2, DOK4, CSF2RB, SCN1A, EVL, ROBO1, PIK3CB*
Cation-coupled Chloride cotransporters	R-HSA-426117	1	7	0.057	0.197	*SLC12A4*
Interactions of neurexins and neuroligins at synapses	R-HSA-6794361	2	57	0.070	0.212	*BEGAIN, SYT10*
Protein-protein interactions at synapses	R-HSA-6794362	2	57	0.070	0.212	*BEGAIN, SYT10*
SALM protein interactions at the synapses	R-HSA-8849932	1	21	0.149	0.284	*LRFN4*
Potassium Channels	R-HSA-1296071	2	99	0.169	0.300	*ABCC8, KCNV2*
Metal ion SLC transporters	R-HSA-425410	1	25	0.174	0.304	*HEPH*
Transmission across Chemical Synapses	R-HSA-112315	3	208	0.201	0.329	*TSPOAP1, PPFIA1, GAD2*
Inwardly rectifying K^+ channels	R-HSA-1296065	1	31	0.209	0.334	*ABCC8*
Vesicle-mediated transport	R-HSA-5653656	6	573	0.251	0.369	*AP1G2, CD163, CFTR, PRKAG2, HIP1R,COG4*
Voltage gated Potassium channels	R-HSA-1296072	1	43	0.276	0.389	*KCNV2*
Cardiac conduction	R-HSA-5576891	2	141	0.281	0.393	*SCN1A, NOS1*
Ion homeostasis	R-HSA-5578775	1	56	0.342	0.439	*NOS1*

Ca^{2+} pathway	R-HSA-4086398	1	61	0.366	0.456	*TCF7L1*

Table 3 Gene-based pathway enrichment according to Reactome (MAF < 0.001)

Pathways	ID	Input number	Background number	*P*-Value	Corrected *P*-Value	Genes
Cardiac conduction	R-HSA-5576891	3	141	0.0246	0.177	*HIPK2, NOS1, ASPH*
Ion homeostasis	R-HSA-5578775	2	56	0.026	0.179	*NOS1, ASPH*
Axon guidance	R-HSA-422475	6	549	0.034	0.191	*COL4A3, EPHB4, PSMB11, COL5A1, EVL, ROBO1*
Ion channel transport	R-HSA-983712	3	211	0.066	0.229	*SLC9B1, ATP2C2, ASPH*
SALM protein interactions at the synapses	R-HSA-8849932	1	21	0.091	0.261	*LRFN4*
Ion transport by P-type ATPases	R-HSA-936837	1	57	0.222	0.379	*ATP2C2*
Transport of inorganic cations/ anions and amino acids/oligopeptides	R-HSA-425393	1	100	0.354	0.486	*SLC26A4*
Neuronal System	R-HSA-112316	1	339	0.771	0.800	*LRFN4*
Vesicle-mediated transport	R-HSA-5653656	1	573	0.918	0.9236	*CD163*

Table 4 Gene-based burden results for candidate genes

Gene	MAF<0.01				MAF<0.001			
	OR	*P* value	Cases	Controls	OR	*P* value	Cases	Controls
CFTR	4.67	4.546E-6	68	51	1.89	2.570E-1	6	4
EVL	NA*	4.352E-5	12	0	NA	4.352E-05	12	0
HIP1R	NA	3.256E-3	7	0	NA	2.016E-1	2	0
ABCC8	NA	7.539E-3	6	0	NA	8.961E-2	3	0
COG4	9.24	1.629E-2	7	1	NA	8.961E-2	3	0
LAMC1	9.24	1.629E-2	7	1	1.22	6.995E-1	1	1
AP1G2	9.24	1.629E-2	7	1	NA	4.505E-1	1	0
GAD2	NA	1.733E-2	5	0	NA	4.505E-1	1	0
CSF2RB	NA	1.733E-2	5	0	NA	2.016E-1	2	0
BEGAIN	NA	1.733E-2	5	0	NA	8.961E-2	3	0
SYT10	NA	1.733E-2	5	0	NA	4.505E-1	1	0
LRFN4	NA	1.733E-2	5	0	NA	1.733E-2	5	0
NOS1	1.95	2.000E-2	42	35	1.93	2.337E-2	39	32
SLC12A4	5.	2.433E-2	8	2	3.18	1.489E-1	5	2
ROBO1	5.30	2.433E-2	8	2	9.24	1.628E-2	7	1
SFTPA2	3.26	2.447E-2	12	5	5.01	9.055E-3	11	3
TSPOAP1	3.99	3.123E-2	9	3	1.66	3.9110E-1	4	3
KCNV2	7.82	3.324E-2	6	1	2.48	4.257E-1	2	1
PIK3CB	7.82	3.324E-2	6	1	2.48	4.257E-1	2	1
CD163	NA	3.955E-2	4	0	NA	3.955E-2	4	0
PRKAG2	NA	3.955E-2	4	0	NA	4.505E-1	1	0
DOK4	NA	3.955E-2	4	0	NA	2.016E-1	2	0
HEPH	NA	3.955E-2	4	0	NA	2.016E-1	2	0
SCN1A	NA	3.955E-2	4	0	NA	8.961E-2	3	0
PPFIA1	NA	3.955E-2	4	0	NA	8.961E-2	3	0
EPHB4	4.57	4.592E-2	7	2	7.82	3.324E-2	6	1
MMP2	4.57	4.592E-2	7	2	5.08	1.284E-1	4	1
TCF3	4.57	4.592E-2	7	2	3.76	2.398E-1	3	1
COL5A1	3.50	5.570E-2	8	3	4.57	4.592E-2	7	2
ATP2C2	2.59	1.046E-1	8	4	7.82	3.324E-2	6	1
SLC26A4	2.55	1.606E-1	6	3	NA	3.955E-2	4	0
ASPH	2.55	1.606E-1	6	3	NA	3.955E-2	4	0
PSMB11	2.24	1.673E-1	7	4	NA	3.955E-2	4	0
RYR2	1.60	2.433E-1	10	8	3.50	5.570E-2	8	3
COL4A3	1.89	2.570E-1	6	4	NA	1.733E-2	5	0
HIPK2	0.94	6.424E-1	7	9	NA	1.733E-2	5	0
SLC9B1		1.00E0	82	100	2.93	3.021E-2	77	84

Note：* NA, not available as the number of cases or controls is zero; MAF, minor allele frequency.

Table 5 PPI network combined scores

Genes	Number of nodes in group 1	Total scores	Mean scores	Number of nodes in group 2	Total scores	Mean scores	Combined mean total scores	Combined mean number of nodes
RYR2	37	23.226	0.628	10	6.533	0.653	14.880	23.5
NOS1	12	9.121	0.760	5	4.469	0.894	6.795	8.5
SCN1A	18	10.844	0.602	3	1.297	0.432	6.071	10.5
CFTR	8	5.596	0.700	5	3.750	0.75	4.673	6.5
EPHB4	4	2.463	0.616	11	6.508	0.592	4.483	7.5
PRKAG2	14	7.370	0.526	2	1.299	0.650	4.335	8
ROBO1	3	1.958	0.653	10	6.524	0.652	4.241	6.5
ASPH	4	3.105	0.776	3	2.897	0.966	3.001	3.5
MMP2	4	2.741	0.685	4	2.589	0.647	2.665	4
ABCC8	8	4.278	0.535	1	0.496	0.496	2.387	4.5
ATP2C2	4	2.077	0.519	5	2.687	0.537	2.382	4.5
COL5A1	3	2.28	0.760	3	2.280	0.760	2.280	3
CSF2RB	2	1.819	0.910	3	2.340	0.780	2.080	2.5
PIK3CB	3	1.977	0.659	2	1.361	0.681	1.669	2.5
COL4A3	3	1.782	0.594	2	1.356	0.678	1.569	2.5
HIPK2	3	2.433	0.811	1	0.625	0.625	1.529	2
SFTPA2	2	1.841	0.921	1	0.917	0.917	1.379	1.5
HIP1R	2	1.800	0.900	1	0.900	0.900	1.350	1.5
EVL	1	0.925	0.925	2	1.503	0.752	1.214	1.5
SLC26A4	2	1.143	0.572	2	1.186	0.593	1.165	2
PPFIA1	1	0.933	0.933	1	0.933	0.933	0.933	1
GAD2	2	0.929	0.465	2	0.929	0.465	0.929	2
PSMB11	1	0.905	0.905	1	0.905	0.905	0.905	1

TCF7L1	1	0.625	0.625	1	0.625	0.625	0.625	1
LAMC1	1	0.553	0.553	1	0.553	0.553	0.553	1
KCNV2	1	0.926	0.926	NA	NA	NA	0.463	0.5
COG4	1	0.902	0.902	NA	NA	NA	0.451	0.5
SLC12A4	1	0.591	0.591	NA	NA	NA	0.296	0.5
SYT10	1	0.400	0.400	NA	NA	NA	0.200	0.5

Notes: group1 means the PPI network was constructed with 36 candidate genes from gene-based collapsing analysis and 64 referential target genes with mutations in the present study; group2 means the PPI network was constructed with 37 candidate genes (including *RYR2*) from gene-based collapsing analysis and 20 selected genes in the top-30 enrichment pathways with both KEGG and Reactome databases in GWAS analysis; NA, not available.

Table 6 The external data validation of candidate genes by the UK Biobank resource

Genes	Start position	End position	Number of Rare variants	MAC-cases	MAC-controls	Cases	Controls	P-value	Phenotype code	Phenotype name
ASPH	8:61503374:G:C	8:61651126:T:C	220	89.00	1663.043487	2570	42728	4.035E-2	427.00	Cardiac dysrhythmias
CD163	12:7479895:T:C	12:7502526:T:C	69	4	150.0004211	95	9405	3.605E-2	426.91	Cardiac pacemaker in situ
CD163	12:7479895:T:C	12:7502526:T:C	79	5	171.00	108	10692	9.246E-3	426.90	Cardiac pacemaker/device in situ
CFTR	7:117480105:C:T	7:117592658:G:A	197	14.00	932.09	95	9405	7.580E-3	426.91	Cardiac pacemaker in situ
COG4	16:70481032:T:C	16:70512433:C:T	62	4	151	93	9207	4.767E-4	427.50	Arrhythmia (cardiac) NOS
CSF2RB	22:36922267:C:A	22:36938476:G:A	92	4	234.00	108	10692	8.011E-3	426.9	Cardiac pacemaker/device in situ
CSF2RB	22:36922267:C:A	22:36938476:G:A	84	4	202.00	95	9405	5.619E-3	426.91	Cardiac pacemaker in situ
CSF2RB	22:36922267:C:A	22:36938476:G:A	79	5	219	104	10296	2.413E-2	427.40	Cardiac arrest and ventricular fibrillation
EPHB4	7:100803517:A:G	7:100826991:C:T	107	10	487.00	116	11484	1.433E-2	425.00	Cardiomyopathy
EPHB4	7:100805215:C:T	7:100826991:C:T	81	5	181.01	78	7722	1.302E-2	427.12	Paroxysmal ventricular tachycardia
GAD2	10:26216843:G:A	10:26245919:A:G	76	17	1590.00	276	27324	1.285E-2	427.11	Paroxysmal supraventricular tachycardia
GAD2	10:26216843:G:A	10:26245919:A:G	85	19	2030.00	354	35046	2.535E-2	427.10	Paroxysmal tachycardia, unspecified
HIP1R	12:122834989:T:C	12:122860524:G:A	144	11	472.00	108	10692	4.155E-3	426.90	Cardiac pacemaker/device in situ
HIP1R	12:122834978:A:C	12:122861041:T:C	291	24.00	1507.01	354	35046	1.837E-2	427.10	Paroxysmal tachycardia, unspecified
HIP1R	12:122834989:T:C	12:122860524:G:A	126	8	355.00	78	7722	2.860E-2	427.12	Paroxysmal ventricular tachycardia
HIP1R	12:122834989:T:C	12:122860524:G:A	249	17.00	1185.01	276	27324	2.887E-2	427.11	Paroxysmal supraventricular tachycardia
HIP1R	12:122834989:T:C	12:122860524:G:A	134	11	418.00	95	9405	1.179E-3	426.91	Cardiac pacemaker in situ
KCNV2	9:2717744:D:4	9:2729710:D:5	88	5.00	199.00	87	8613	4.110E-3	427.42	Cardiac arrest
KCNV2	9:2717744:D:4	9:2729710:D:5	91	5.00	218.00	104	10296	4879553E-3	427.40	Cardiac arrest and ventricular fibrillation
MMP2	16:55479557:C:A	16:55505425:G:A	53	2	91.00	78	7722	4.910E-2	427.12	Paroxysmal ventricular tachycardia
NOS1	12:117218074:T:C	12:117278099:C:G	272	143.00	3398.00	1468	42760	1.183E-2	427.20	Atrial fibrillation and flutter
PIK3CB	3:138655414:G:A	3:138759288:G:A	95	5	213.00	276	27324	3.915E-2	427.11	Paroxysmal supraventricular tachycardia
PPFIA1	11:70272251:C:G	11:70382137:C:G	73	3	137.00	78	7722	4.004E-2	427.12	Paroxysmal ventricular tachycardia
PRKAG2	7:151557224:G:A	7:151675419:C:T	38	2	51	78	7722	1.452E-2	427.12	Paroxysmal ventricular tachycardia
PRKAG2	7:151557224:G:A	7:151595452:C:T	36	4	52.00	87	8613	1.868E-4	427.42	Cardiac arrest
PRKAG2	7:151557224:G:A	7:151595452:C:T	41	4	62.00	104	10296	2.122E-4	427.40	Cardiac arrest and ventricular fibrillation

ROBO1	3:78600114:T:A	3:79018406:C:T	344	56.00	1702.02	1468	42760	2.524E-3	427.20	Atrial fibrillation and flutter
ROBO1	3:78600114:T:A	3:79018406:C:T	350	92.01	1700.02	2570	42728	1.813E-2	427.00	Cardiac dysrhythmias
ROBO1	3:78600114:T:A	3:78598929:T:C	118	8.00	344.01	93	9207	3.817E-2	427.50	Arrhythmia (cardiac) NOS
SCN1A	2:165991287:T:G	2:166041470:C:A	85	6	274.02	104	10296	3.253E-4	427.40	Cardiac arrest and ventricular fibrillation
SCN1A	2:165991287:T:G	2:166041470:C:A	69	6	225.02	87	8613	1.139E-4	427.42	Cardiac arrest
SLC9B1	4:102901162:A:T	4:102991714:T:C	47	17	736.01	104	10296	2.837E-2	427.40	Cardiac arrest and ventricular fibrillation
SYT10	12:33376837:G:A	12:33439521:A:G	46	3	97.00	116	11484	1.042E-2	425.00	Cardiomyopathy

Note: MAC: Minor allele counts.

Table 7 Candidate Genes Enrichment Analysis for Phenotype Category in UK Biobank (p<0.05)

Phenotype category name	Enrichment *P* value	-Log10(*P* value)	Category name	Phenotype code
Paroxysmal supraventricular tachycardia	0.000174146	3.759	circulatory system	427.11
Paroxysmal tachycardia, unspecified	0.009124029	2.040	circulatory system	427.1
Aneurysm and dissection of heart	0.01165878	1.933	circulatory system	411.41
Other hypertrophic and atrophic conditions of skin	0.007023506	2.153	dermatologic	701
Nephritis; nephrosis; renal sclerosis	0.010817149	1.966	genitourinary	580
Intestinal infection due to C. difficile	0.0137383	1.862	infectious diseases	008.52
Anaphylactic shock NOS	0.014210121	1.847	injuries & poisonings	946
Opiates and related narcotics causing adverse effects in therapeutic use	0.01073407	1.969	injuries & poisonings	965.1
Bacterial pneumonia	0.008187189	2.087	respiratory	480.1

Table 8 Overlapped candidates gene mutations in an AVNRT study from Denmark

Our Present Study									Danish AVNRT Study							
Gene	Hgv.c	Hgv.p	Triscript	Functions	KG_EAS_AF	ExAC_EAS_AF	cases(N)	controls(N)	Gene	cDNA	Protein variant	Transcript	Translation	MAF ExAC	MAF D2K*	Allele count
RYR2	***c.4652A>G***	***p.Asn1551Ser***	***XM_005273224.1***	***missense***	**.**	***4.52E-03***	***1***	***0***	***RYR2***	***c.4652A>G***	***p.Asn1551Ser***	***ENST00000366574***	***missense***	***3.50E-04***	***5.00E-04***	***1***
	c.4094C>T	p.Ala1365Val	XM_005273224.1	missense	7.90E-03	4.21E-03	2	4		c.1088T>C	p.Ile363Thr	ENST00000366574	missense	0.00	0.00	1
	c.7076G>A	p.Arg2359Gln	XM_005273224.1	missense	.	7.00E-04	1	0		c.1115T>A	p.Leu372His	ENST00000366574	missense	1.00E-05	2.50E-04	1
	c.3143A>G	p.Asp1048Gly	XM_005273224.1	missense	.	.	1	0		c.1250G>A	p.Arg417Gln	ENST00000366574	missense	2.00E-05	0.00E+00	2
	c.6040G>T	p.Asp2014Tyr	XM_005273224.1	missense	.	.	1	0		c.2828T>C	p.Leu943Ser	ENST00000366574	missense	2.30E-04	0.00E+00	1
	c.5774T>C	p.Ile1925Thr	XM_005273224.1	missense	.	0.00	1	0		c.3251G>A	p.Arg1084Lys	ENST00000366574	missense	1.50E-04	7.50E-04	1
	c.11352T>G	p.Ile3784Met	XM_005273224.1	missense	.	.	1	0		c.5186T>C	p.Met1729Thr	ENST00000366574	missense	0.00	0.00	1
	c.13050A>C	p.Leu4350Phe	XM_005273224.1	missense	.	.	0	1		c.8162T>C	p.Ile2721Thr	ENST00000366574	missense	5.70E-04	4.13E-03	1
	c.5923A>G	p.Met1975Val	XM_005273224.1	missense	.	2.34E-04	0	1		c.10468G>T	p.Ala3490Ser	ENST00000366574	missense	0.00E+00	2.50E-04	1
	c.5570C>T	p.Pro1857Leu	XM_005273224.1	missense	0.00	1.17E-46	1	0		c.10528C>A	p.Arg3510Ser	ENST00000366574	missense	3.00E-05	2.50E-04	1
	c.6092C>T	p.Ser2031Phe	XM_005273224.1	missense	.	1.16E-04	1	0		c.10846G>T	p.Ala36165er	ENST00000366574	missense	0.00	0.00	1
	c.3683C>A	p.Thr1228Asn	XM_005273224.1	missense	.	.	1	1		.	.	.	.	.	.	.
	c.3721G>A	p.Val1241Ile	XM_005273224.1	missense	2.00E-03	2.33E-04	0	1		.	.	.	.	.	.	.
SCN1A	c.3176A>T	p.Asp1059Val	NM_001165963.1	missense	.	3.52E-08	1	0	**SCN1A**	c.3521C>G	p.Thr11745er	ENST00000303395	missense	1.77E-03	3.25E-03	2
	c.3053G>A	p.Arg1018Lys	NM_001165963.1	missense	.	2.32E-08	1	0		c.1625G>A	p.Arg542Gln	ENST00000303395	missense	1.53E-03	1.75E-03	1
	c.2141T>G	p.Met714Arg	NM_001165963.1	missense	.	.	1	0		c.1199T>C	p.Met400Thr	ENST00000303395	missense	0.00	0.00	1
	c.135C>G	p.Asp45Glu	NM_001165963.1	missense	1.00E-03	8.09E-04	1	0		.	.	.	.	.	.	.

MAFD2K: 2000 Danish Exomes; ExAC, Exome Aggregation Consortium; MAF, minor allel frequency; NA, not available.